

Article

Phytochemical Composition and Detection of Novel Bioactives in Anther Callus of *Catharanthus roseus* L.

Yashika Bansal ¹, A. Mujib ^{1,*}, Jyoti Mangain ¹, Yaser Hassan Dewir ² and Hail Z. Rihan ³

¹ Cellular Differentiation and Molecular Genetics Section, Department of Botany, Jamia Hamdard, New Delhi 110062, India; yashikab333@gmail.com (Y.B.); jyotimangain93@gmail.com (J.M.)

² Plant Production Department, College of Food and Agriculture Sciences, King Saud University, Riyadh 11451, Saudi Arabia; ydewir@ksu.edu.sa

³ School of Biological and Marine Sciences, Faculty of Science and Engineering, University of Plymouth, Drake Circus PL4 8AA, UK; hail.rihan@plymouth.ac.uk

* Correspondence: amujib3@yahoo.co.in

Abstract: *Catharanthus roseus* L. (G.) Don is the most widely studied plant because of its high pharmacological value. In vitro culture uses various plant parts such as leaves, nodes, internodes and roots for inducing callus and subsequent plant regeneration in *C. roseus*. However, till now, little work has been conducted on anther tissue using plant tissue culture techniques. Therefore, the aim of this work is to establish a protocol for in vitro induction of callus by utilizing anthers as explants in MS (Murashige and Skoog) medium fortified with different concentrations and combinations of PGRs. The best callusing medium contains high α -naphthalene acetic acid (NAA) and low kinetin (Kn) concentrations showing a callusing frequency of 86.6%. SEM–EDX analysis was carried out to compare the elemental distribution on the surfaces of anther and anther-derived calli, and the two were noted to be nearly identical in their elemental composition. Gas chromatography–mass spectrometry (GC–MS) analysis of methanol extracts of anther and anther-derived calli was conducted, which revealed the presence of a wide range of phytochemicals. Some of them are ajmalicine, vindoline, coronaridine, squalene, pleiocarpamine, stigmaterol, etc. More importantly, about 17 compounds are exclusively present in anther-derived callus (not in anther) of *Catharanthus*. The ploidy status of anther-derived callus was examined via flow cytometry (FCM), and it was estimated to be 0.76 pg, showing the haploid nature of callus. The present work therefore represents an efficient way to produce high-value medicinal compounds from anther callus in a lesser period of time on a larger scale.

Keywords: anther culture; flow cytometry; GC–MS; phytochemical profiling; ploidy level; secondary metabolites; SEM–EDX



Citation: Bansal, Y.; Mujib, A.; Mangain, J.; Dewir, Y.H.; Rihan, H.Z. Phytochemical Composition and Detection of Novel Bioactives in Anther Callus of *Catharanthus roseus* L. *Plants* **2023**, *12*, 2186. <https://doi.org/10.3390/plants12112186>

Academic Editor: Ain Raal

Received: 12 May 2023

Revised: 29 May 2023

Accepted: 29 May 2023

Published: 31 May 2023



Copyright: © 2023 by the authors. Licensee MDPI, Basel, Switzerland. This article is an open access article distributed under the terms and conditions of the Creative Commons Attribution (CC BY) license (<https://creativecommons.org/licenses/by/4.0/>).

1. Introduction

Catharanthus roseus (L.) G. Don, a member of the Apocynaceae family, is a popular flowering plant. It is an indigenous species to Madagascar and is widely distributed throughout the African, American, Asian and southern European regions. In India, *C. roseus* has been spread across all the major parts of Gujarat, Madhya Pradesh, Assam, Bihar, Uttar Pradesh, Karnataka and Tamil Nadu [1]. The plant is well known for both its ornamental and medicinal value. It produces nearly 130 alkaloids, of which vincristine and vinblastine are the two major compounds that are used in the treatment of leukemia and Hodgkin's lymphoma [2]. For decades, this plant has been exploited for pharmaceutically active compounds from its native environments and thus is at risk of declining in the wild. Plant tissue culture proves to be an effective biotechnological tool for the rapid propagation of plants under aseptic conditions with a lesser risk of microbial infections [3]. Several in vitro studies using different explants have been successfully conducted for somatic embryogenesis [4] and organogenesis in *C. roseus* [5,6].

In recent times, double haploid (DH) production via anther is a promising option for developing improved plant varieties with high yields of medicinally important bioactive compounds [7]. In vitro anther culture has been attempted in various plants such as *Actinidia arguta* Planch [8] and *Triticum aestivum* L. [9]. Various factors such as stage of anther, culture conditions, plant growth regulators (PGRs) and genotypic and ploidy status determine the success of DH generation [10]. These factors necessitate ascertaining the ploidy status of anther-derived callus to generate true-to-type DH lines, which can be performed with a flow cytometric technique. The flow cytometry method (FCM) measures the genome size by examining the nuclei at a relatively faster rate and thus validates the ploidy levels of different plant tissues [11]. Recent investigations of genome size analysis using FCM have been reported for different plants [12,13]. Phytochemical profiling using gas chromatography coupled with mass spectrometry (GC–MS) has emerged as an important procedure for identifying and quantifying therapeutically significant compounds present in medicinal plants. This technique is relatively faster, accurate and needs a minimum volume of extracts to detect a wide range of bioactive compounds such as alkaloids, long-chain hydrocarbons, steroids, sugars, amino acids and nitro compounds [14]. Major bioactive compounds extracted from different plant parts of *C. roseus* such as stem, root and leaf include vincristine, vinblastine, reserpine, ajmalicine, vindoline and catharine, which possess anti-cancerous, anti-diabetic, anti-fungal and anti-microbial activities [15]. GC–MS-based profiling has been recently reported for several plants including *Silybum marianum* L. [16] and *Chukrasia velutina* [17], but the information on tissue-culture-raised plants' phytochemical profiling is relatively much less. The present work, therefore, focuses on investigating the ploidy status of anther-derived callus of *C. roseus* using flow cytometry. The elemental composition of both anther and anther calli was studied using a scanning electron microscopy–energy-dispersive X-ray microanalysis (SEM–EDX) technique. The identification of the bioactive compounds present in methanolic extracts of anther and anther-derived calli was conducted for the first time in *C. roseus* using GC–MS analysis. This report will help to understand and improve the yield of the important pharmaceutical compounds synthesized from anther-derived callus.

2. Results

2.1. Callus Induction and Proliferation

In this study, the anthers were used as explants to induce callus on MS medium augmented with different concentrations and combinations of NAA and kinetin or TDZ alone (Figure 1A). The callusing response ranged from 13.3% to 86.6% on all the tested media (Table 1). Among the PGRs utilized, a combination of NAA and kinetin produced maximum callus (86.6%) at concentrations of 1.0 mg/L and 0.1 mg/L, respectively, followed by 0.75 mg/L TDZ with a frequency of 73.3%. On the other hand, TDZ alone at 0.5 mg/L showed the least incidence of callusing efficiency (13.3%). The highest callus fresh weight was noted to be 1.7 g on MS medium containing 1.0 mg/L NAA and 0.1 mg/L kinetin. The calli obtained were white to pale yellow in color and friable in nature (Figure 1B–D). The anther callus was noted to be recalcitrant, as plant regeneration (embryogenesis and organogenesis) was not achieved on any medium added with various PGR combinations.

Table 1. Effect of different concentrations and combinations of PGRs on callus induction and callus biomass (fresh weight) from anther explants of *C. roseus*.

PGRs	Concentration (mg/L)	Callusing Frequency (%)	Mean Fresh Weight (g)
Control	0	0 ^e	0 ^c
NAA + Kn	0.1 + 1.0	26.6 ± 12.4 ^{cde}	0.8 ± 0.3 ^{abc}
	0.5 + 0.75	33.3 ± 14.9 ^{cde}	0.9 ± 0.3 ^{ab}
	0.75 + 0.5	53.3 ± 16.9 ^{abc}	1.1 ± 0.3 ^{ab}
	1.0 + 0.1	86.6 ± 8.1 ^a	1.7 ± 1.7 ^a

Table 1. Cont.

PGRs	Concentration (mg/L)	Callusing Frequency (%)	Mean Fresh Weight (g)
TDZ	0.5	13.3 ± 8.1 ^{de}	0.5 ± 0.3 ^{bc}
	0.75	73.3 ± 27.8 ^{ab}	1.3 ± 0.2 ^{ab}
	1	46.6 ± 16.9 ^{bcd}	0.9 ± 0.2 ^{ab}

Mean values followed by the same superscripts within a column are not significantly different according to DMRT at $p \leq 0.05$ level.

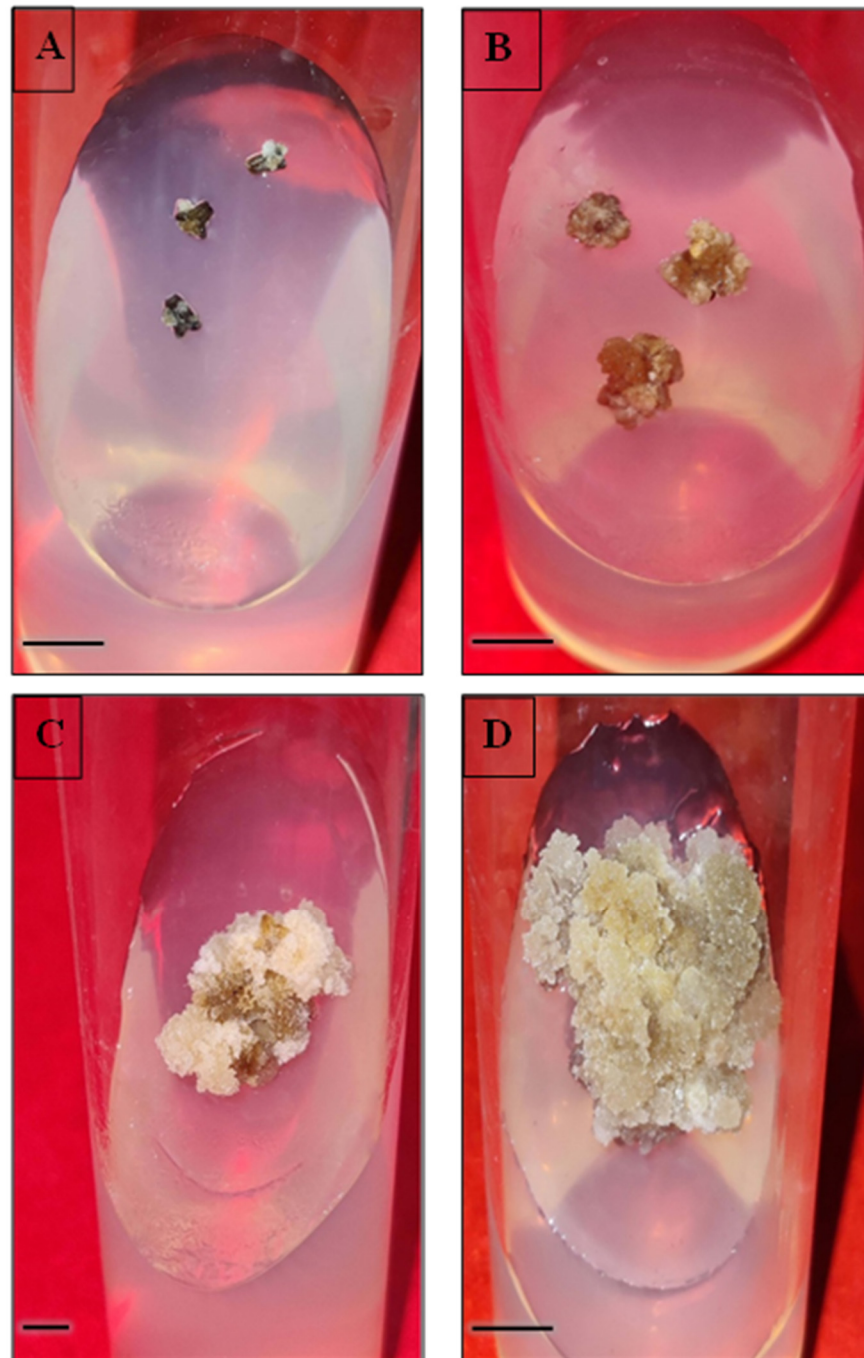


Figure 1. Cont.

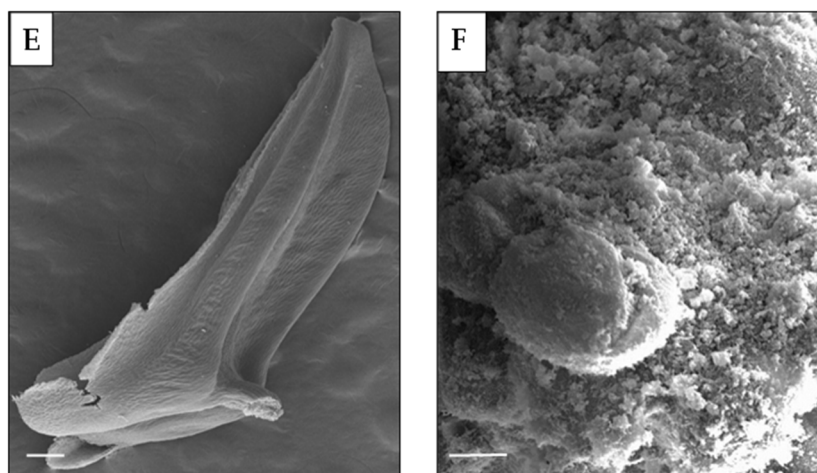


Figure 1. In vitro callus induction, proliferation and scanning electron microscopic (SEM) images of anther and anther-derived callus of *C. roseus*. (A,B): callus initiation (bars = 0.5 cm); (C,D): callus proliferation after 6 and 9 weeks, respectively (bars (C) = 1.0 cm, (D) = 0.5 cm); (E): side view of anther (bar = 200 μ m); (F): a portion of anther-derived callus (bar = 20 μ m).

2.2. Surface Morphology and Elemental Analysis

SEM–EDAX analysis was carried out to determine the elemental composition of anther as well as anther-derived callus. The SEM images and their respective spectra are shown in Figure 1E,F and Figure 2, respectively. The various peaks in both spectra reveal carbon, oxygen, sodium and phosphorous to be the major elements present on the surfaces of anther and anther-derived calli. In both the samples, the carbon and oxygen peaks are prominent and of high intensity, whereas those of sodium and phosphorous are of nearly equal intensity. The quantitative estimation of elements is presented in Table 2.

Table 2. Elemental composition of anther and anther-derived callus of *C. roseus* using SEM–EDX analysis.

S.No.	Element	Anther Explant		Anther-Derived Callus	
		Weight %	Atomic %	Weight %	Atomic %
1	Carbon	33.59	70.67	47.34	79.42
2	Oxygen	12.65	19.97	11.55	14.55
3	Sodium	1.93	2.12	1.63	1.42
4	Phosphorous	0.87	0.71	1.03	0.67

2.3. GC–MS Analysis

The bioactive compounds present in methanolic extracts of anthers (donor material) and anther-derived callus of *C. roseus* (Figure 3) were identified using the GC–MS technique. The active principles with their retention time (RT), peak area % (concentration), molecular formula and molecular weight from the NIST library are presented in Tables 3 and 4, and the GC–MS chromatograms are presented in Figure 4A,B. The chromatograms reveal more than 50 phytochemicals in both methanolic extracts belonging to various classes such as terpenoids, phenols, lignans, steroids, alkaloids and fatty acids.

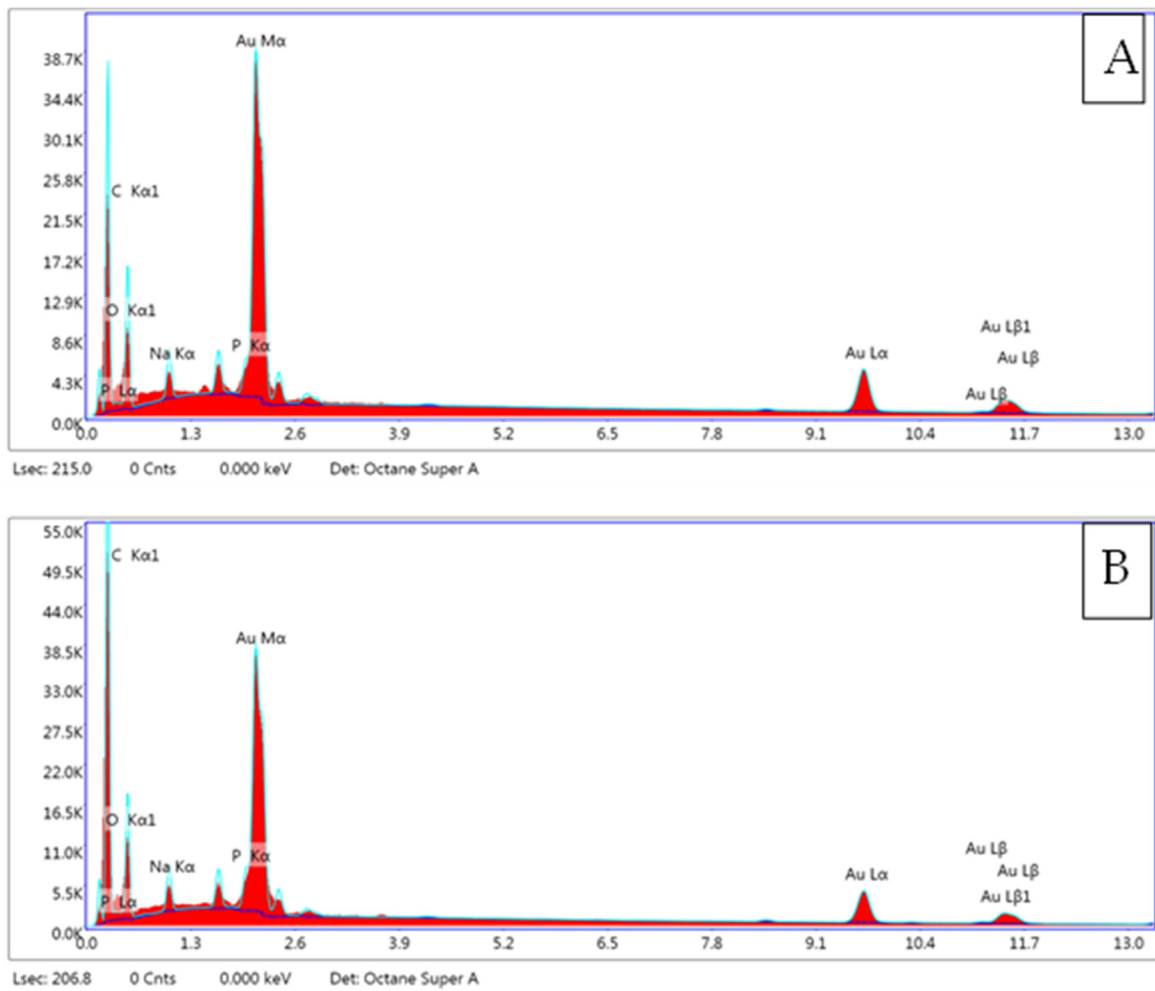


Figure 2. SEM–EDX analysis micrographs showing elemental composition of *C. roseus*. (A): field grown anther; (B): anther-derived callus.

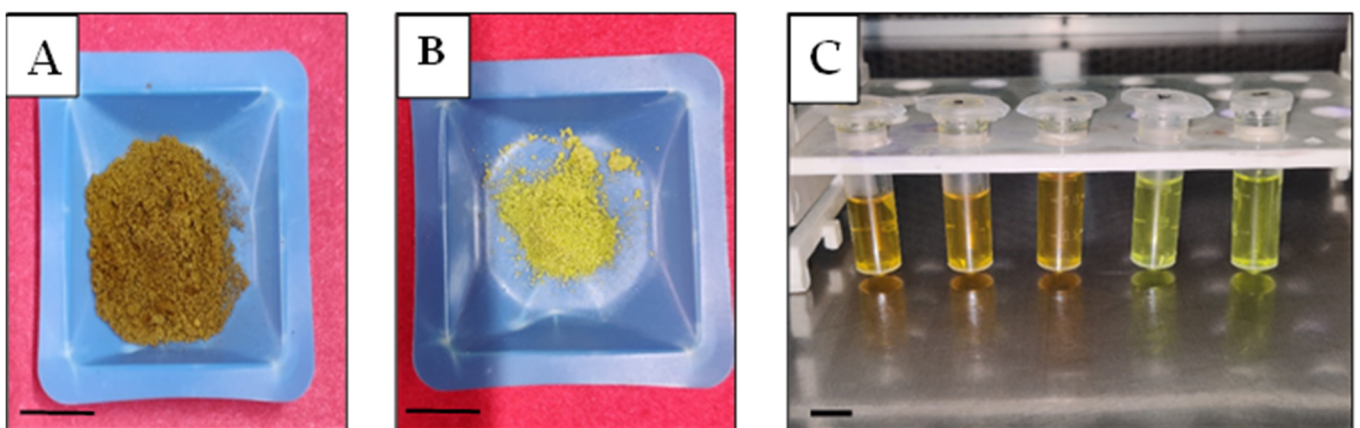


Figure 3. Extract preparation for GC–MS analysis of *C. roseus*. (A): dried powder of anther-derived callus; (B): dried powder of field-grown anther; (C): methanolic extracts of the samples (A,B).

Table 3. List of phytochemicals identified in the methanolic extract of field-grown anther of *C. roseus* using GC–MS analysis.

S.No.	RT (min)	Peak Area %	Name of the Compound	Molecular Formula	Molecular Weight
1	3.760	1.62	Ethylcyclopentenolone	C ₇ H ₁₀ O ₂	126
2	4.436	1.12	Pyranone	C ₆ H ₈ O ₄	144
3	5.484	1.17	Coumaran	C ₈ H ₈ O	120
4	5.739	0.42	1-monoacetin	C ₅ H ₁₀ O ₄	134
5	6.287	0.26	6-oxoheptanoic acid	C ₇ H ₁₂ O ₃	144
6	6.504	0.38	Indole	C ₈ H ₇ N	117
7	6.628	0.14	4-vinylguaiaicol	C ₉ H ₁₀ O ₂	150
8	7.616	2.12	1,2-octanediol	C ₈ H ₁₈ O ₂	146
9	9.101	18.42	Guanosine	C ₁₀ H ₁₃ N ₅ O ₅	283
10	9.816	0.45	2,6-dimethoxy-4-vinylphenol	C ₁₀ H ₁₂ O ₃	180
11	10.086	0.78	1,2-benzenedicarboxylic acid, diethyl ester	C ₁₂ H ₁₄ O ₄	222
12	10.473	0.09	Cedrol	C ₁₅ H ₂₆ O	222
13	10.796	0.17	Dihydromethyljasmonate	C ₁₃ H ₂₂ O ₃	226
14	11.050	3.78	Quinic acid	C ₇ H ₁₂ O ₆	192
15	11.914	0.08	2-benzylideneoctanal	C ₁₅ H ₂₀ O	216
16	12.061	2.86	Mome inositol	C ₇ H ₁₄ O ₆	194
17	13.082	0.13	Diisobutyl phthalate	C ₁₆ H ₂₂ O ₄	278
18	13.411	0.11	Heptadecane	C ₁₇ H ₃₆	240
19	13.681	0.09	Methyl palmitate	C ₁₇ H ₃₄ O ₂	270
20	14.117	0.18	n-hexadecanoic acid	C ₁₆ H ₃₂ O ₂	256
21	14.403	0.12	Eicosane	C ₂₀ H ₄₂	282
22	15.355	4.71	Hexacosane	C ₂₆ H ₅₄	366
23	15.883	0.09	Docosanoic acid	C ₂₂ H ₄₄ O ₂	340
24	16.259	0.79	Tetracosane	C ₂₄ H ₅₀	338
25	16.910	0.35	9-tricosanol acetate	C ₂₅ H ₅₀ O ₂	382
26	17.134	9.78	Hexatriacontane	C ₃₆ H ₇₄	506
27	17.293	0.20	4,5-dihydro-2-[(8Z,11Z)-8,11-heptadecadienyl]oxazole	C ₂₀ H ₃₅ NO	305
28	17.398	0.19	4,8-cyclododecadien-1-one	C ₁₂ H ₁₈ O	178
29	17.963	1.13	Dotriacontane	C ₃₂ H ₆₆	450
30	18.571	0.30	Octacosanol	C ₂₈ H ₅₈ O	410
31	18.765	2.82	n-tetracontane	C ₄₀ H ₈₂	562
32	18.953	0.80	alpha-monostearin	C ₂₁ H ₄₂ O ₄	358
33	19.536	0.22	1-bromotriacontane	C ₃₀ H ₆₁ Br	500
34	20.322	0.11	Linoleyl acetate	C ₂₀ H ₃₆ O ₂	308
35	20.523	0.12	(-)-Coronaridine	C ₂₁ H ₂₆ N ₂ O ₂	338
36	21.137	27.01	Squalene	C ₃₀ H ₅₀	410
37	22.759	0.19	Arachidic acid, 3-methylbutyl ester	C ₂₅ H ₅₀ O ₂	382
38	22.896	0.57	beta-tocopherol	C ₂₈ H ₄₈ O ₂	416

Table 3. *Cont.*

S.No.	RT (min)	Peak Area %	Name of the Compound	Molecular Formula	Molecular Weight
39	23.543	0.30	Vitamin E	C ₂₉ H ₅₀ O ₂	430
40	24.640	1.20	Campesterol	C ₂₈ H ₄₈ O	400
41	24.766	0.30	Ergostan-3-ol	C ₂₈ H ₅₀ O	402
42	25.105	0.08	Trans-24-ethylidenecholesterol	C ₂₉ H ₄₈ O	412
43	25.178	0.52	3-oxocholestane	C ₂₇ H ₄₆ O	386
44	25.440	0.22	p-coumaric acid, 2-methylpropyl ether, 2-methylpropyl ester	C ₁₇ H ₂₄ O ₃	276
45	25.603	2.87	gamma-sitosterol	C ₂₉ H ₅₀ O	414
46	25.762	0.57	Stigmastanol	C ₂₉ H ₅₂ O	416
47	26.055	0.16	Ergosta-4,24(28)-dien-3-one	C ₂₈ H ₄₄ O	396
48	26.132	0.87	4-campesterene-3-one	C ₂₈ H ₄₆ O	398
49	26.230	0.23	Cholestanone	C ₂₇ H ₄₆ O	386
50	27.321	2.72	Methyl commate C	C ₃₁ H ₅₀ O ₄	486
51	28.021	5.54	alpha amyryn	C ₃₀ H ₅₀ O	426

Table 4. List of phytochemicals identified in the methanolic extract of anther-derived callus of *C. roseus* using GC-MS analysis.

S.No.	RT (min)	Peak Area %	Name of the Compound	Molecular Formula	Molecular Weight
1	3.598	0.58	1,3,5-triazine-2,4,6-triamine	C ₃ H ₆ N ₆	126
2	4.320	0.10	Isopropylmethylnitrosamine	C ₄ H ₁₀ N ₂ O	102
3	4.498	5.49	1,2,3-propanetriol	C ₃ H ₈ O ₃	92
4	5.040	0.23	3-cis-methoxy-5-trans-methyl-1R-cyclohexanol	C ₈ H ₁₆ O ₂	144
5	5.270	0.35	Catechol	C ₆ H ₆ O ₂	110
6	5.402	0.50	2,5,5-trimethylhepta-2,6-dien-4-ol	C ₁₀ H ₁₈ O	154
7	5.508	3.89	5-hydroxymethylfurfural	C ₆ H ₆ O ₃	126
8	5.735	1.06	1-monoacetin	C ₅ H ₁₀ O ₄	134
9	5.949	0.15	Decanoic acid	C ₁₀ H ₂₀ O ₂	172
10	6.304	0.40	4-oxopentyl acetate	C ₇ H ₁₂ O ₃	144
11	7.133	0.24	Eugenol acetate	C ₁₂ H ₁₄ O ₃	206
12	8.022	0.07	Indan-1,3-diol monoacetate	C ₁₁ H ₁₂ O ₃	192
13	8.728	6.16	Guanosine	C ₁₀ H ₁₃ N ₅ O ₅	283
14	9.764	0.08	Dodecanoic acid	C ₁₂ H ₂₄ O ₂	200
15	10.784	0.15	Dihydromethyljasmonate	C ₁₃ H ₂₂ O ₃	226
16	10.986	0.10	1-(4-isopropylphenyl)-2-methylpropyl acetate	C ₁₅ H ₂₂ O ₂	234
17	11.145	0.27	Benzoic acid, 2-hydroxy-, heptyl ester	C ₁₄ H ₂₀ O ₃	236
18	11.555	0.19	Methyl myristate	C ₁₅ H ₃₀ O ₂	242
19	11.934	0.61	4-((1E)-3-hydroxy-1-propenyl)-2-methoxyphenol	C ₁₀ H ₁₂ O ₃	180

Table 4. Cont.

S.No.	RT (min)	Peak Area %	Name of the Compound	Molecular Formula	Molecular Weight
20	12.030	0.11	Tridecanoic acid	C ₁₃ H ₂₆ O ₂	214
21	12.246	0.20	Stearic acid methyl ester	C ₁₉ H ₃₈ O ₂	298
22	12.334	0.72	Octadecanoic acid, methyl ester	C ₁₉ H ₃₈ O ₂	298
23	12.640	0.14	Pentadecanoic acid, methyl ester	C ₁₆ H ₃₂ O ₂	256
24	13.075	0.29	Diisobutyl phthalate	C ₁₆ H ₂₂ O ₄	278
25	13.255	0.03	1-hexadecanol	C ₁₆ H ₃₄ O	242
26	13.298	0.62	Hexadecanoic acid, methyl ester	C ₁₇ H ₃₄ O ₂	270
27	13.467	0.19	Methyl palmitoleate	C ₁₇ H ₃₂ O ₂	268
28	13.580	0.03	7,9-di-tert-butyl-1-oxaspiro(4,5)deca-6,9-diene-2,8-dione	C ₁₇ H ₂₄ O ₃	276
29	13.676	3.96	Methyl palmitate	C ₁₇ H ₃₄ O ₂	270
30	14.113	0.21	n-hexadecanoic acid	C ₁₆ H ₃₂ O ₂	256
31	14.305	0.49	Decyl hexofuranoside	C ₁₆ H ₃₂ O ₆	320
32	14.387	0.50	Eicosanoic acid, methyl ester	C ₂₁ H ₄₂ O ₂	326
33	14.533	0.36	Cis-sinapyl alcohol	C ₁₁ H ₁₄ O ₄	210
34	14.664	0.15	Heptadecanoic acid, methyl ester	C ₁₈ H ₃₆ O ₂	284
35	14.925	0.12	Oxybenzone	C ₁₄ H ₁₂ O ₃	228
36	15.316	3.31	Linoleic acid, methyl ester	C ₁₉ H ₃₄ O ₂	294
37	15.374	1.97	Ethyl oleate	C ₂₀ H ₃₈ O ₂	310
38	15.423	0.72	Oleic acid, methyl ester	C ₁₉ H ₃₆ O ₂	296
39	15.607	0.79	Octadecanoic acid, methyl ester	C ₁₉ H ₃₈ O ₂	298
40	16.399	0.70	cis-10-nonadecenoic acid, methyl ester	C ₂₀ H ₃₈ O ₂	310
41	16.816	0.08	4,8,13-duvatriene-1,3-diol	C ₂₀ H ₃₄ O ₂	306
42	17.290	0.08	4,5-dihydro-2-[(8Z,11Z)-8,11-heptadecadienyl]oxazole	C ₂₀ H ₃₅ NO	305
43	17.335	0.03	(Z)-2-(pentadec-8-en-1-yl)-4,5-dihydrooxazole	C ₁₈ H ₃₃ NO	279
44	17.379	0.16	Methyl arachidate	C ₂₁ H ₄₂ O ₂	326
45	17.589	0.45	6-methyladenine, TMS derivative	C ₉ H ₁₅ N ₅ Si	221
46	17.888	0.09	Octadecanoic acid, 2,3-dihydroxypropyl ester	C ₂₁ H ₄₂ O ₄	358
47	18.239	0.15	Henicosanal	C ₂₁ H ₄₂ O	310
48	18.746	0.12	Nonadecylpentafluoropropionate	C ₂₂ H ₃₉ F ₅ O ₂	430
49	18.948	0.21	alpha-monostearin	C ₂₁ H ₄₂ O ₄	358
50	19.006	0.28	Docosanoic acid, methyl ester	C ₂₃ H ₄₆ O ₂	354
51	19.522	0.21	Vindolinine	C ₂₁ H ₂₄ N ₂ O ₂	336
52	19.775	0.12	Methyl tricosanoate	C ₂₄ H ₄₈ O ₂	368
53	20.046	0.09	Octocrylene	C ₂₄ H ₂₇ NO ₂	361
54	20.317	0.25	n-propyl linoleate	C ₂₁ H ₃₈ O ₂	322
55	20.593	0.10	Pleiocarpamine	C ₂₀ H ₂₂ N ₂ O ₂	322
56	21.122	0.89	Squalene	C ₃₀ H ₅₀	410

Table 4. Cont.

S.No.	RT (min)	Peak Area %	Name of the Compound	Molecular Formula	Molecular Weight
57	22.404	0.36	(+)-Pericyclivine	C ₂₀ H ₂₂ N ₂ O ₂	322
58	22.793	0.47	Ajmalicine	C ₂₁ H ₂₄ N ₂ O ₃	352
59	23.162	0.20	Cholesta-4,6-dien-3-ol	C ₂₇ H ₄₄ O	384
60	23.470	0.24	Ajmalicine oxindole	C ₂₁ H ₂₄ N ₂ O ₄	368
61	24.641	1.69	Campesterol	C ₂₈ H ₄₈ O	400
62	24.901	1.23	Stigmasta-5,20(22)-dien-3-ol	C ₂₉ H ₄₈ O	412
63	25.035	0.84	19-epiajmalicine	C ₂₁ H ₂₄ N ₂ O ₃	352
64	25.187	5.32	3-oxocholestane	C ₂₇ H ₄₆ O	386
65	25.476	2.09	beta-stigmasterol	C ₂₉ H ₄₈ O	412
66	25.600	2.42	gamma-sitosterol	C ₂₉ H ₅₀ O	414
67	25.790	1.76	(E)-1-(6,10-dimethylundec-5-en-2-yl)-4-methylbenzene	C ₂₀ H ₃₂	272
68	25.990	0.30	(22E)-ergosta-4,7,22-trien-3-one	C ₂₈ H ₄₂ O	394
69	26.137	4.88	4-campestene-3-one	C ₂₈ H ₄₆ O	398
70	26.235	4.62	Cholestanone	C ₂₇ H ₄₆ O	386
71	26.459	4.47	Stigmasterone	C ₂₉ H ₄₆ O	410
72	26.547	0.22	6-dehydroprogesterone	C ₂₁ H ₂₈ O ₂	312
73	26.640	0.56	Cycloartenol	C ₃₀ H ₅₀ O	426
74	26.776	0.20	3,5-cholestadien-7-one	C ₂₇ H ₄₂ O	382
75	26.869	0.61	Ergosta-4,6,22-trien-3-one	C ₂₈ H ₄₂ O	394
76	27.336	7.08	gamma-sitostenone	C ₂₉ H ₄₈ O	412
77	27.448	1.97	24-methylenecycloartanol	C ₃₁ H ₅₂ O	440
78	27.806	0.93	Stigmasta-3,5-dien-7-one	C ₂₉ H ₄₆ O	410
79	28.442	5.87	4,4-dimethylcholestan-3-one	C ₂₉ H ₅₀ O	414
80	28.846	3.78	(22E)-4-methylstigmast-22-en-3-one	C ₃₀ H ₅₀ O	426
81	30.011	5.55	3-acetylcholestan-2-one	C ₂₉ H ₄₈ O ₂	428

Among the compounds identified, 1-monoacetin, guanosine, dihydromethyljasmonate, n-hexadecanoic acid, squalene, campesterol, cholestanone and gamma-sitosterol were the most prevalent present in both extracts. Only the methanolic extract of anthers contained bioactives such as cedrol (0.09%), (-)-coronaridine (0.12%), 4-vinylguaiaicol (0.14%), vitamin E (0.30%), stigmastanol (0.57%), quinic acid (3.78%) and alpha amyryl (5.54%) (Table 3), and their respective mass spectra are shown in Figure S1A. The extract of anther-derived calli was found to have characteristic metabolites such as pleiocarpamine (0.10%), vindoline (0.21%), cis-sinapyl alcohol (0.36%), (+)-pericyclivine (0.36%), ajmalicine (0.47%), cycloartenol (0.56%) and beta-stigmasterol (2.09%) (Tables 4 and 5) having specific mass spectra (Figure S1B).

2.4. Flow Cytometric Analysis

The ploidy status of callus obtained from anther was determined using a flow cytometric approach wherein good quality nuclei are a necessity. In this study, the leaves of field-grown *C. roseus* were utilized as an external standard reference (control). The flow cytometric histogram peak of callus reveals that its DNA content was nearly half to that of its diploid counterpart (control) (Figure 5A,B). The nuclear DNA content of anther-derived

cell/callus was 0.76 pg compared to the diploid leaves' DNA (1.51 pg) with a DNA Index (DI) of 0.51 (Table 6). This estimation confirms the haploid DNA status of callus obtained from anther.

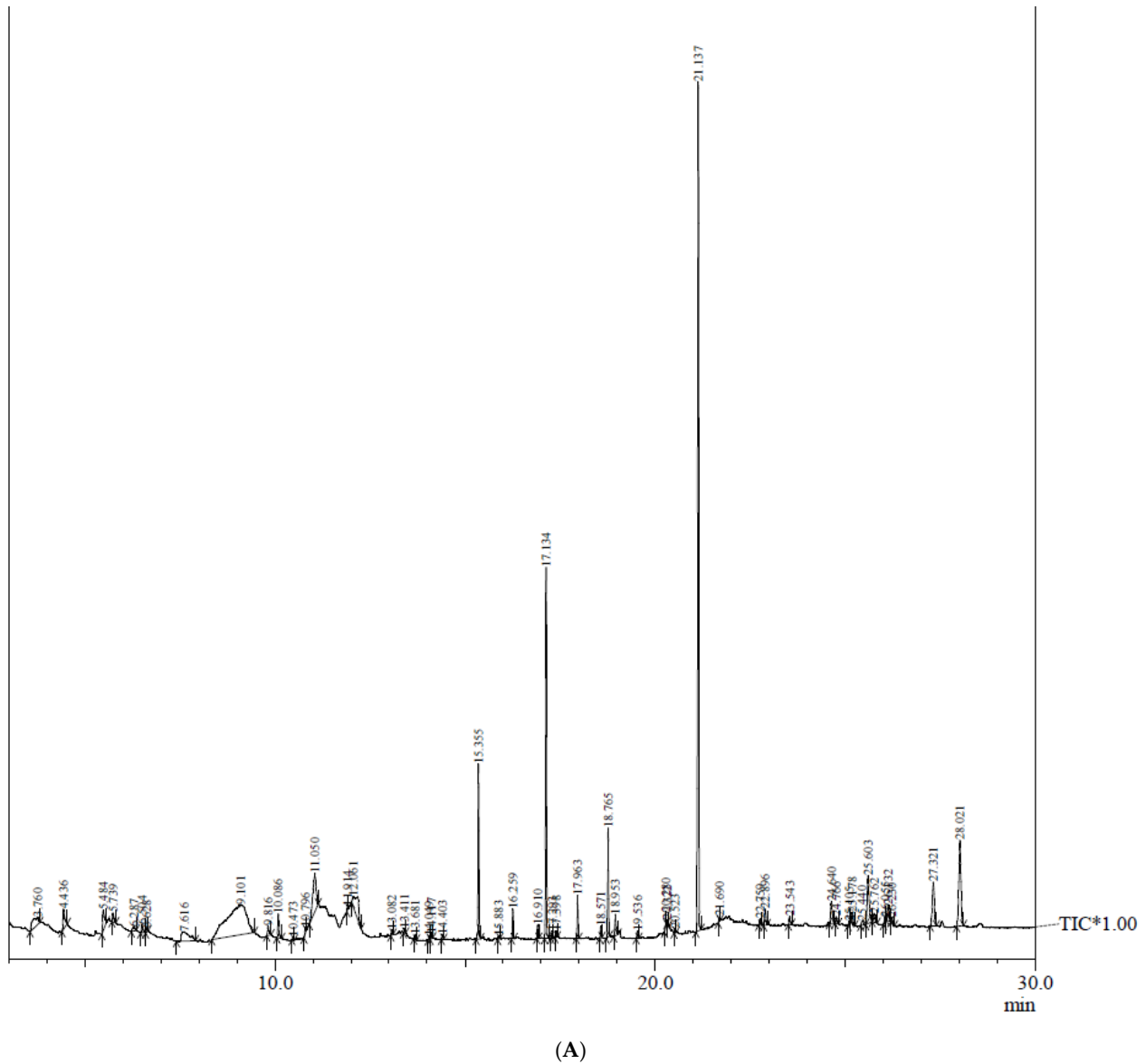


Figure 4. Cont.

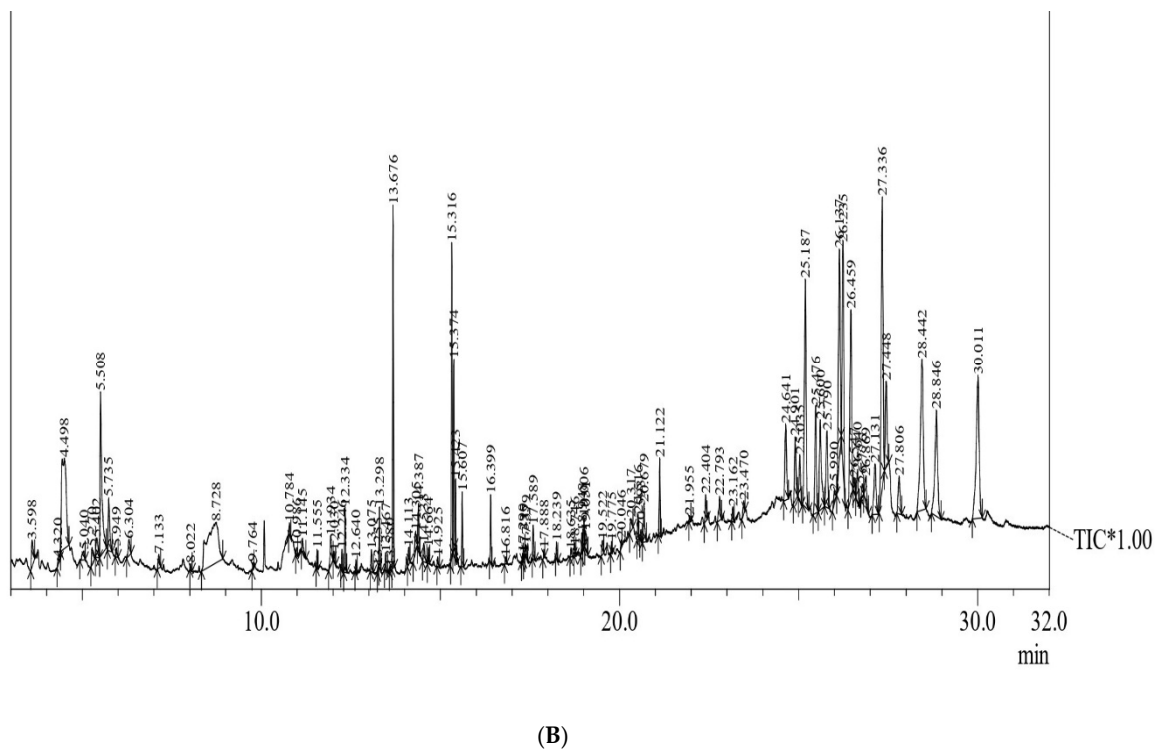


Figure 4. (A): GC–MS chromatogram (total ionic chromatogram) of methanolic extract of anthers of *C. roseus*; (B): GC–MS chromatogram (total ionic chromatogram) of methanolic extract of anther-derived callus of *C. roseus*.

Table 5. List of important phytochemicals identified exclusively in the methanolic extract of anther-derived callus of *C. roseus* using GC–MS analysis.

S.No.	RT (min)	Name of the Compound	Molecular Formula
1	7.133	Eugenol acetate	C ₁₂ H ₁₄ O ₃
2	12.246	Stearic acid methyl ester	C ₁₉ H ₃₈ O ₂
3	14.533	Cis-sinapyl alcohol	C ₁₁ H ₁₄ O ₄
4	14.925	Oxybenzone	C ₁₄ H ₁₂ O ₃
5	15.316	Linoleic acid, methyl ester	C ₁₉ H ₃₄ O ₂
6	15.423	Oleic acid, methyl ester	C ₁₉ H ₃₆ O ₂
7	19.522	Vindoline	C ₂₁ H ₂₄ N ₂ O ₂
8	20.046	Octocrylene	C ₂₄ H ₂₇ NO ₂
9	20.593	Pleiocarpamine	C ₂₀ H ₂₂ N ₂ O ₂
10	22.404	(+)-Pericyclivine	C ₂₀ H ₂₂ N ₂ O ₂
11	22.793	Ajmalicine	C ₂₁ H ₂₄ N ₂ O ₃
12	25.035	19-epiajmalicine	C ₂₁ H ₂₄ N ₂ O ₃
13	25.476	beta-stigmasterol	C ₂₉ H ₄₈ O
14	26.459	Stigmasterone	C ₂₉ H ₄₆ O
15	26.547	6-dehydroprogesterone	C ₂₁ H ₂₈ O ₂
16	26.640	Cycloartenol	C ₃₀ H ₅₀ O
17	27.336	gamma-sitosterone	C ₂₉ H ₄₈ O

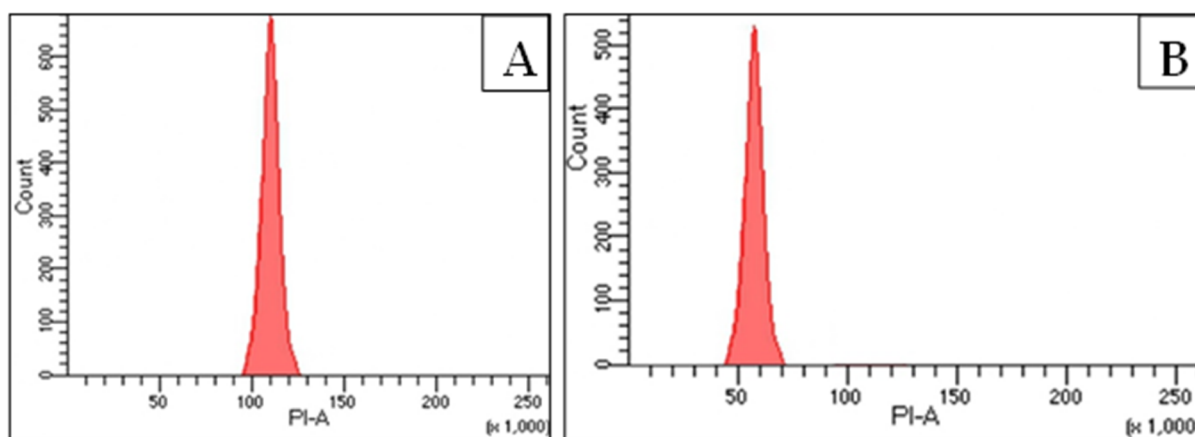


Figure 5. Flow cytometric histograms revealing ploidy level of (A) diploid leaves of *C. roseus* (standard) and (B) anther-derived callus of *C. roseus*.

Table 6. Estimation of nuclear DNA content, genome size and DNA index of anther-derived callus with respect to donor plant of *C. roseus* using flow cytometry technique.

Plant Sample Type	Nuclear DNA Content (pg)	Genome Size (Mbp) *	DNA Index (DI) **
Standard (leaves)	1.51	1476.7	-
Anther-derived callus	0.76	743.2	0.51

* 1 pg = 978 Mbp [18]. ** DNA Index = sample DNA content/standard DNA content.

3. Discussion

The present work was conducted to evaluate the callusing potentiality of anthers of *C. roseus* under in vitro culture conditions. The type and concentration of PGRs used in media strongly affect callusing ability and are different in different plant species. Initially, the anthers were subject to different concentrations and combinations of PGRs amended in MS medium. The results indicate that a high-to-low ratio of auxin: cytokinin concentrations was proven to be the best in inducing callus with a maximum mean fresh weight, which is very similar to Kou et al.'s [19] and Rout et al.'s [20] observations. Likewise, TDZ alone at different concentrations was found to be equally effective in producing callus and subsequent proliferation. Previous reports suggested that TDZ (a cytokinin-like PGR) alone may be used in improving callusing ability in different explants [21,22]. A comparison of the elemental distribution on the surfaces of anther and anther-derived callus was performed using SEM–EDX analysis, revealing a nearly similar elemental composition on both samples. EDX analyzes X-rays emitted from samples receiving a high-energy electron beam. This technique facilitates the qualitative and semi-quantitative detection of surface elements of samples and has been extensively used on various plant species such as sesame [23] and lemongrass [24].

Medicinal plants are an ingenious source of bioactive compounds that fight against several chronic diseases, and these phytochemicals can be identified and quantified using the GC–MS technique [25]. In the current study, phytochemical profiling with GC–MS of methanolic extracts (Figure 5) of anther and anther-derived callus of *C. roseus* has been conducted. The results obtained show the presence of various phytoconstituents, including carbohydrates, alkaloids, phenols, saponins, phytosterols, terpenoids, steroids, etc. A total of 14 bioactives are common in both the extracted samples. However, there are compounds that are exclusive to each sample that confer various biological properties to this plant. The presence of secondary metabolites in callus, which are otherwise not detected in anther tissue, may be due to the fact that certain bioactive compounds accumulate in specific cells or tissues or in a specific growth stage (mostly the stationary phase) of in vitro cultures [26]. Therefore, developing callus from different tissues to obtain therapeutically active compounds is of high significance.

The major compounds of medicinal value present in the methanolic extract of anthers were squalene (triterpene), alpha-amyrin (triterpene), coronaridine (alkaloid) and cedrol (essential oil), which possess anti-oxidant, gastroprotective and hepatoprotective, anti-cancerous and anti-inflammatory properties, respectively [27–30]. Similarly, in anther-derived calli exclusively, 17 compounds are present having diverse medicinal properties, and these compounds are listed in Table 5. These include stearic acid, linoleic acid, oleic acid, vindolinine, pleiocarpamine, pericyclivine, ajmalicine, 19-epiajmalicine, beta-stigmasterol, cycloartenol, etc. Ajmalicine and vindolinine are well-known alkaloids having anti-cancerous, anti-hypertensive and anti-oxidant properties [15,31]. Recently, an alkaloid named pleiocarpamine has been isolated from the stem bark of *Rauvolfia caffra* and is reported to possess anti-seizure activity [32]. Cycloartenol (a triterpenoid) and stigmasterol (a sterol) have also been detected in present studies and are associated with immunosuppressive, anti-hypercholesterolemic and anti-inflammatory activities, respectively [33,34]. Compounds such as cycloartenol, ajmalicine, vindolinine, pleiocarpamine and pericyclivine have been reported previously in leaf tissues of *C. roseus* [35,36]. Some reports of phyto-compounds identified from different tissues using GC–MS were noted earlier [37,38], but till now, no information on the phyto-compounds present in anther or anther-derived callus was available for *C. roseus*.

The ploidy status of anther-derived callus was checked using flow cytometry, and the results show that the ploidy of the calli was haploid in nature, confirming the involvement of microspores in developing callus. Similar observations have also been reported for other plant species [7,10,39]. FCM is the widely used approach for determining the ploidy of plants developed through callus, somatic embryos and other in vitro-regenerated pathways [40]. The origin of diploid plants from anthers may be due to the involvement of other somatic cells such as anther wall, filament or flower septum in developing callus. Spontaneous chromosomal doubling can also be a mechanism in the generation of polyploidy in anther-derived regenerants. In certain cases, mixoploids and aneuploids have also been noted in anther cultures of different plants [8,41], but these polyploids were not detected in this experiment. This is the first-ever report of GC–MS analysis of medically significant compounds from anther tissue of *C. roseus*, which enriches the phyto-compound library of *Catharanthus* and may be utilized in the pharmaceutical and industrial sectors.

4. Materials and Methods

4.1. Anther Culture and Growth Conditions

The mature flowers of *C. roseus* were collected from the herbal garden, Jamia Hamdard, New Delhi, and the anthers were used as explants for experimentations. The surface sterilization of flowers was performed following the method of Bansal et al. [3] described earlier. The sterilized anthers were excised from the flowers and aseptically cultured onto agar-solidified basal Murashige and Skoog (MS) medium supplemented with various concentrations and combinations of plant growth regulators (PGRs) and sub-cultured every 3–4 weeks. The cultures were incubated at a temperature of 24 ± 2 °C with $48 \mu\text{mol}/\text{m}^2/\text{s}^2$ illumination (white fluorescent light) for a 16 h photoperiod.

4.2. Callus Induction and Proliferation

The disinfected anthers were inoculated on MS augmented with different concentrations (alone or in combination) of α -naphthalene acetic acid (NAA), kinetin (Kn) and thidiazuron (TDZ) ranging from 0.1 to 1.0 mg/L for callus induction. Callus formation started within 14–16 days of culture and proliferated on the same medium with successive subculturing. The callus induction frequency and the callus fresh weight were recorded after 6 weeks of culture.

$$\text{Callus induction frequency (\%)} = \frac{\text{Number of explants showing callusing}}{\text{Total number of explants inoculated}} \times 100$$

4.3. Surface Morphology and Elemental Analysis

The surface morphology and elemental profile of anther and anther-derived callus were determined using energy-dispersive X-ray microanalysis (EDX) combined with scanning electron microscopy (SEM). For this purpose, the samples were primarily fixed with Karnovsky's fixative and washed with 0.1 M phosphate buffer at 4 °C. Afterward, a series of dehydrations with acetone (30%, 50%, 70%, 90% and 100%) were performed at 15 min intervals, and then critical-point drying was performed at 1100 p.s.i. These samples were then mounted on aluminum stubs and sputter-coated with gold having a 35 nm thick film. Finally, the coated samples were viewed at an accelerating voltage of 20 kV under a scanning electron microscope (Zeiss, Oberkochen, Germany) equipped with EDAX.

4.4. Preparation of Extracts

The methanolic extracts of both samples were prepared according to the protocol of Hussain et al. [42]. About 1.0 g of anther and anther callus were shade dried and crushed into fine powder using mortar and pestle (Figure 3A,B). Each sample was then extracted in 5.0 mL methanol in an orbital shaker for 48 h. Afterward, the extracts were filtered through Whatman filter paper no. 1 and evaporated to dryness. The obtained extracts were stored in an airtight container with proper labeling at 4 °C for further use (Figure 3C).

4.5. GC-MS Analysis

GC-MS analyses of these extracts were conducted on GC-MS QP-2010 equipment (Shimadzu, Japan) at Advanced Instrumentation Research Facility (AIRF), JNU, New Delhi. The program settings were as follows: Helium was used as a carrier gas (1 mL/min), and the initial and final temperatures were programmed at 100 °C and 260 °C, respectively, with a hold time of 18 min. Ion source temperature was 220 °C with an interface temperature of 270 °C and solvent cut time of 2.5 min. Other specifications included: detector gain mode relative to the tuning result, detector gain +0.00 kV, threshold of 1000, start time 3 min, end time 39.98 min, event time 0.3 s, scan speed of 2000, start m/z 40.00 and end m/z 600.00.

4.6. Metabolite Data Processing and Analysis

The bioactive compounds were identified using the mass spectral database of the NIST17 library. The unknown compounds' spectra were compared with the known phytochemical spectra available in the NIST library, and the name, molecular weight and structure of the compounds were determined.

4.7. Flow Cytometric Analysis

The ploidy status of anther-derived calli was examined using the flow cytometry method as described by Galbraith [43]. A total of 3 samples of anther-derived callus were randomly chosen, along with a reference standard of diploid leaves of *C. roseus* with a known 2C DNA content of 1.51 pg [44]. Approximately 50 mg of callus was added to a Petri plate having 1.0 mL ice-cold Galbraith's buffer (nuclei isolation buffer) and finely macerated with the help of a surgical blade. The homogenate was then filtered with a 100 µm nylon mesh to eliminate larger cellular remnants and was finally stained with 50 µg/mL PI RNase (propidium iodide RNase) (Sigma-Aldrich, St. Louis, MO, USA) for 8–10 min. The samples were incubated in the dark at 4 °C for about 40 min and eventually examined on a BD FACS(Calibur) flow cytometer (BD Biosciences, Franklin Lakes, NJ, USA). The relative nuclear DNA of anther-derived callus of *C. roseus* was estimated using the below formula [45]:

$$\text{Nuclear DNA content of sample (pg)} = 2\text{C DNA content of standard (pg)} \times \frac{\text{mean position of G0/G1 peak of sample}}{\text{mean position of G0/G1 peak of standard}}$$

4.8. Statistical Analysis

In the tissue-culture experiment, three explants (anthers) per culture tube were inoculated with five replicates of every experimental treatment, and each experiment was

repeated twice. The data are expressed as mean \pm standard error, and the analysis was performed using one-way analysis of variance (ANOVA). The significance of mean difference was determined using Duncan's multiple range test (DMRT) at $p < 0.05$ using SPSS Ver. 26.0 (SPSS Inc., Chicago, IL, USA) [46]. The flow cytometric study was repeated thrice with randomly chosen standard (donor plant) and callus samples.

5. Conclusions

The in vitro culture technology was successfully employed to obtain callus from anther tissue of *C. roseus*, an important medicinal plant. The callus was checked for its ploidy status using flow cytometry and was found to be haploid in nature. The calli obtained from anther were then subjected to GC–MS analysis for phytochemical identification. Among the bioactive compounds identified, ajmalicine, vindoline, pleiocarpamine, pericyclivine, stigmaterol, campesterol and squalenes were detected and have a wide range of biological activities. From this study, it can then be concluded that anther-derived calli are a potent source for developing new therapeutic drugs with larger-scale applicability in pharmaceutical sectors.

Supplementary Materials: The following supporting information can be downloaded at: <https://www.mdpi.com/article/10.3390/plants12112186/s1>, Figure S1A,B: Mass spectra of identified compounds from methanolic extract of anthers and anther derived callus of *C. roseus*.

Author Contributions: Conceptualization, A.M. and Y.B.; methodology, Y.B.; formal analysis, Y.B.; investigation, Y.B.; data curation, Y.B.; writing—original draft preparation, Y.B.; writing—review and editing, Y.B., A.M., J.M., Y.H.D. and H.Z.R.; validation, Y.H.D. and H.Z.R.; visualization, Y.H.D. and H.Z.R.; supervision, A.M.; project administration, A.M. All authors have read and agreed to the published version of the manuscript.

Funding: This research work is funded by the Department of Biotechnology (DBT), New Delhi, India (DBT/2020/JH/1336).

Institutional Review Board Statement: Not applicable.

Informed Consent Statement: Not applicable.

Data Availability Statement: All data are presented in the article.

Acknowledgments: The first author is thankful to the Department of Biotechnology (DBT) for the financial support given in the form of the Junior Research Fellowship and to AIRF, JNU, New Delhi, for providing the GC–MS facility. The authors are grateful for the laboratory facilities provided by the Department of Botany, Jamia Hamdard, New Delhi. The authors acknowledge Researchers Supporting Project number (RSP2023R375), King Saud University, Riyadh, Saudi Arabia.

Conflicts of Interest: The authors declare no conflict of interest.

Abbreviations

PGRs	Plant Growth Regulators
MS	Murashige and Skoog
NAA	α -Naphthaleneacetic acid
Kn	Kinetin
TDZ	Thidiazuron
DH	Double Haploid
SEM–EDX	Scanning Electron Microscopy–Energy-Dispersive X-ray
FCM	Flow Cytometric Method
DI	DNA Index
GC–MS	Gas Chromatography–Mass Spectrometry
DMRT	Duncan's Multiple Range Test

References

1. Das, A.; Sarkar, S.; Bhattacharyya, S.; Gantait, S. Biotechnological advancements in *Catharanthus roseus* (L.) G. Don. *Appl. Microbiol. Biotechnol.* **2020**, *10*, 44811–44835. [\[CrossRef\]](#)
2. Dhayanithy, G.; Subban, K.; Chelliah, J. Diversity and biological activities of endophytic fungi associated with *Catharanthus roseus*. *BMC Microbiol.* **2019**, *19*, 1–14. [\[CrossRef\]](#) [\[PubMed\]](#)
3. Bansal, Y.; Mujib, A.; Siddiqui, Z.H.; Mamgain, J.; Syeed, R.; Ejaz, B. Ploidy status, nuclear DNA content and start codon targeted (SCoT) genetic homogeneity assessment in *Digitalis purpurea* L., regenerated in vitro. *Genes* **2022**, *13*, 2335. [\[CrossRef\]](#) [\[PubMed\]](#)
4. Mujib, A.; Bansal, Y.; Malik, M.Q.; Syeed, R.; Mamgain, J.; Ejaz, B. Internal and external regulatory elements controlling somatic embryogenesis in *Catharanthus*: A model medicinal plant. In *Somatic Embryogenesis, Methods in Molecular Biology*; Ramirez-Mosqueda, M.A., Ed.; Humana: New York, NY, USA, 2022; Volume 2527, pp. 11–27. [\[CrossRef\]](#)
5. Dhandapani, M.; Kim, D.H.; Hong, S.B. Efficient plant regeneration via somatic embryogenesis and organogenesis from the explants of *Catharanthus roseus*. *In Vitro Cell. Dev. Biol. Plant* **2008**, *44*, 18–25. [\[CrossRef\]](#)
6. Verma, P.; Mathur, A.K. Direct shoot bud organogenesis and plant regeneration from pre-plasmolysed leaf explants in *Catharanthus roseus*. *Plant Cell Tissue Organ Cult.* **2011**, *106*, 401–408. [\[CrossRef\]](#)
7. Hoveida, Z.S.; Abdollahi, M.R.; Mirzaie-Asl, A.; Moosavi, S.S.; Seguí-Simarro, J.M. Production of doubled haploid plants from anther cultures of borage (*Borago officinalis* L.) by the application of chemical and physical stress. *Plant Cell Tissue Organ Cult.* **2017**, *130*, 369–378. [\[CrossRef\]](#)
8. Wang, G.F.; Qin, H.Y.; Sun, D.; Fan, S.T.; Yang, Y.M.; Wang, Z.X.; Xu, P.L.; Zhao, Y.; Liu, Y.X.; Ai, J. Haploid plant regeneration from hardy kiwifruit (*Actinidia arguta* Planch.) anther culture. *Plant Cell Tissue Organ Cult.* **2018**, *134*, 15–28. [\[CrossRef\]](#)
9. Abd El-Fatah, B.E.; Sayed, M.A.; El-Sanusy, S.A. Genetic analysis of anther culture response and identification of QTLs associated with response traits in wheat (*Triticum aestivum* L.). *Mol. Biol. Rep.* **2020**, *47*, 9289–9300. [\[CrossRef\]](#)
10. Sahoo, S.A.; Jha, Z.; Verulkar, S.B.; Srivastava, A.K.; Suprasanna, P. High-throughput cell analysis based protocol for ploidy determination in anther-derived rice callus. *Plant Cell Tissue Organ Cult.* **2019**, *137*, 187–192. [\[CrossRef\]](#)
11. Ejaz, B.; Mujib, A.; Mamgain, J.; Malik, M.Q.; Syeed, R.; Gulzar, B.; Bansal, Y. Comprehensive in vitro regeneration study with SCoT marker assisted clonal stability assessment and flow cytometric genome size analysis of *Carthamus tinctorius* L.: An important medicinal plant. *Plant Cell Tissue Organ Cult.* **2022**, *148*, 403–418. [\[CrossRef\]](#)
12. Bhusare, B.P.; John, C.K.; Bhatt, V.P.; Nikam, T.D. Induction of somatic embryogenesis in leaf and root explants of *Digitalis lanata* Ehrh.: Direct and indirect method. *S. Afr. J. Bot.* **2020**, *130*, 356–365. [\[CrossRef\]](#)
13. Mamgain, J.; Mujib, A.; Ejaz, B.; Gulzar, B.; Malik, M.Q.; Syeed, R. Flow cytometry and start codon targeted (SCoT) genetic fidelity assessment of regenerated plantlets in *Tylophora indica* (Burm. f.) Merrill. *Plant Cell Tissue Organ Cult.* **2022**, *150*, 129–140. [\[CrossRef\]](#)
14. Konappa, N.; Udayashankar, A.C.; Krishnamurthy, S.; Pradeep, C.K.; Chowdappa, S.; Jogaiah, S. GC–MS analysis of phytoconstituents from *Amomum nilgircicum* and molecular docking interactions of bioactive serverogenin acetate with target proteins. *Sci. Rep.* **2020**, *10*, 16438. [\[CrossRef\]](#)
15. Pham, H.N.; Vuong, Q.V.; Bowyer, M.C.; Scarlett, C.J. Phytochemicals derived from *Catharanthus roseus* and their health benefits. *Technology* **2020**, *8*, 80. [\[CrossRef\]](#)
16. Padma, M.; Ganesan, S.; Jayaseelan, T.; Azhagumadhavan, S.; Sasikala, P.; Senthilkumar, S.; Mani, P. Phytochemical screening and GC–MS analysis of bioactive compounds present in ethanolic leaves extract of *Silybum marianum* (L.). *J. Drug. Deliv. Ther.* **2019**, *9*, 85–89. [\[CrossRef\]](#)
17. Jahan, I.; Tona, M.R.; Sharmin, S.; Sayeed, M.A.; Tania, F.Z.; Paul, A.; Chy, M.N.; Rakib, A.; Emran, T.B.; Simal-Gandara, J. GC-MS phytochemical profiling, pharmacological properties, and in silico studies of *Chukrasia velutina* leaves: A novel source for bioactive agents. *Molecules* **2020**, *25*, 3536. [\[CrossRef\]](#)
18. Dolezel, J. Nuclear DNA content and genome size of trout and human. *Cytom. Part A* **2003**, *51*, 127–128.
19. Kou, Y.; Ma, G.; Teixeira da Silva, J.A.; Liu, N. Callus induction and shoot organogenesis from anther cultures of *Curcuma attenuata* Wall. *Plant Cell Tissue Organ Cult.* **2013**, *112*, 1–7. [\[CrossRef\]](#)
20. Rout, P.; Naik, N.; Ngangkham, U.; Verma, R.L.; Katara, J.L.; Singh, O.N.; Samantaray, S. Doubled Haploids generated through anther culture from an elite long duration rice hybrid, CRHR32: Method optimization and molecular characterization. *Plant Biotechnol.* **2016**, *33*, 177–186. [\[CrossRef\]](#)
21. Cappelletti, R.; Sabbadini, S.; Mezzetti, B. The use of TDZ for the efficient in vitro regeneration and organogenesis of strawberry and blueberry cultivars. *Sci. Hortic.* **2016**, *207*, 117–124. [\[CrossRef\]](#)
22. Khan, T.; Abbasi, B.H.; Khan, M.A.; Shinwari, Z.K. Differential effects of thidiazuron on production of anticancer phenolic compounds in callus cultures of *Fagonia indica*. *Appl. Biochem. Biotechnol.* **2016**, *179*, 46–58. [\[CrossRef\]](#)
23. Nath, B.; Kalita, P.; Das, B.; Basumatary, S. Highly efficient renewable heterogeneous base catalyst derived from waste *Sesamum indicum* plant for synthesis of biodiesel. *Renew. Energy* **2020**, *151*, 295–310. [\[CrossRef\]](#)
24. Pandey, J.; Sarkar, S.; Verma, R.K.; Singh, S. Sub-cellular localization and quantitative estimation of heavy metals in lemongrass plants grown in multi-metal contaminated tannery sludge. *S. Afr. J. Bot.* **2020**, *131*, 74–83. [\[CrossRef\]](#)
25. Mamgain, J.; Mujib, A.; Syeed, R.; Ejaz, B.; Malik, M.Q.; Bansal, Y. Genome size and gas chromatography-mass spectrometry (GC–MS) analysis of field-grown and in vitro regenerated *Pluchea lanceolata* plants. *J. Appl. Genet.* **2022**, *64*, 1–21. [\[CrossRef\]](#)

26. Leng, T.C.; Ping, N.S.; Lim, B.P.; Keng, C.L. Detection of bioactive compounds from *Spilanthes acmella* (L.) plants and its various in vitro culture products. *J. Med. Plant Res.* **2011**, *5*, 371–378.
27. Diab, M.; Ibrahim, A.; Hadad, G. B. Review article on chemical constituents and biological activity of *Olea europaea*. *Rec. Pharm. Biomed. Sci.* **2020**, *4*, 36–45. [[CrossRef](#)]
28. Nogueira, A.O.; Oliveira, Y.I.S.; Adjafre, B.L.; de Moraes, M.E.A.; Aragão, G.F. Pharmacological effects of the isomeric mixture of alpha and beta amyirin from *Protium heptaphyllum*: A literature review. *Fundam. Clin. Pharmacol.* **2019**, *33*, 4–12. [[CrossRef](#)] [[PubMed](#)]
29. Naidoo, C.M.; Naidoo, Y.; Dewir, Y.H.; Murthy, H.N.; El-Hendawy, S.; Al-Suhaibani, N. Major bioactive alkaloids and biological activities of *Tabernaemontana* species (*Apocynaceae*). *Plants* **2021**, *10*, 313. [[CrossRef](#)] [[PubMed](#)]
30. Özek, G.; Schepetkin, I.A.; Yermagambetova, M.; Özek, T.; Kirpotina, L.N.; Almerikova, S.S.; Abugalieva, S.I.; Khlebnikov, A.I.; Quinn, M.T. Innate immunomodulatory activity of cedrol, a component of essential oils isolated from *Juniperus* species. *Molecules* **2021**, *26*, 7644. [[CrossRef](#)]
31. Hemmati, N.; Azizi, M.; Spina, R.; Dupire, F.; Arouei, H.; Saeedi, M.; Laurain-Mattar, D. Accumulation of ajmalicine and vinblastine in cell cultures is enhanced by endophytic fungi of *Catharanthus roseus* cv. Icy Pink. *Ind. Crops Prod.* **2020**, *158*, 112776. [[CrossRef](#)]
32. Chipiti, T.; Viljoen, A.M.; Cordero-Maldonado, M.L.; Veale, C.G.; Van Heerden, F.R.; Sandasi, M.; Chen, W.; Crawford, A.D.; Enslin, G.M. Anti-seizure activity of African medicinal plants: The identification of bioactive alkaloids from the stem bark of *Rauvolfiacaffra* using an in vivo zebrafish model. *J. Ethnopharmacol.* **2021**, *279*, 114282. [[CrossRef](#)]
33. Bakrim, S.; Benkhaira, N.; Bourais, I.; Benali, T.; Lee, L.-H.; El Omari, N.; Sheikh, R.A.; Goh, K.W.; Ming, L.C.; Bouyahya, A. Health Benefits and Pharmacological Properties of Stigmasterol. *Antioxidants* **2022**, *11*, 1912. [[CrossRef](#)] [[PubMed](#)]
34. Lun, W.U.; Zhi-Li, C.H.; Yang, S.U.; Qiu-Hong, W.A.; Kuang, H.X. Cycloartenol triterpenoid saponins from *Cimicifuga simplex* (*Ranunculaceae*) and their biological effects. *China J. Nat. Med.* **2015**, *13*, 81–89. [[CrossRef](#)]
35. Murata, J.; Roepke, J.; Gordon, H.; De Luca, V. The leaf epidermome of *Catharanthus roseus* reveals its biochemical specialization. *Plant Cell* **2008**, *20*, 524–542. [[CrossRef](#)]
36. Wesołowska, A.; Grzeszczuk, M.; Wilas, J.; Kulpa, D. Gas chromatography-mass spectrometry (GC-MS) analysis of indole alkaloids isolated from *Catharanthus roseus* (L.) G. don cultivated conventionally and derived from in vitro cultures. *Not. Bot. Horti Cluj-Napoca* **2016**, *44*, 100–106. [[CrossRef](#)]
37. Syeda, A.M.; Riazunnisa, K. Data on GC-MS analysis, in vitro anti-oxidant and anti-microbial activity of the *Catharanthus roseus* and *Moringa oleifera* leaf extracts. *Data Brief* **2020**, *29*, 105258. [[CrossRef](#)] [[PubMed](#)]
38. Rani, S.; Singh, V.; Sharma, M.K.; Sisodia, R. GC-MS based metabolite profiling of medicinal plant-*Catharanthus roseus* under cadmium stress. *Plant Physiol. Rep.* **2021**, *26*, 491–502. [[CrossRef](#)]
39. Eshaghi, Z.C.; Abdollahi, M.R.; Moosavi, S.S.; Deljou, A.; Seguí-Simarro, J.M. Induction of androgenesis and production of haploid embryos in anther cultures of borage (*Borago officinalis* L.). *Plant Cell Tissue Organ Cult.* **2015**, *122*, 321–329. [[CrossRef](#)]
40. Gulzar, B.; Mujib, A.; Mushtaq, Z.; Malik, M.Q. Old *Catharanthus roseus* culture (14 years) produced somatic embryos and plants and showed normal genome size; demonstrated an increased antioxidant defense mechanism; and synthesized stress proteins as biochemical, proteomics, and flow-cytometry studies reveal. *J. Appl. Genet.* **2021**, *62*, 43–57. [[CrossRef](#)]
41. Jia, Y.; Zhang, Q.X.; Pan, H.T.; Wang, S.Q.; Liu, Q.L.; Sun, L.X. Callus induction and haploid plant regeneration from baby primrose (*Primula forbesii* Franch.) anther culture. *Sci. Hortic.* **2014**, *176*, 273–281. [[CrossRef](#)]
42. Hussain, S.A.; Ahmad, N.; Anis, M.; Alatar, A.A. Influence of meta-topolin on in vitro organogenesis in *Tecoma stans* L., assessment of genetic fidelity and phytochemical profiling of wild and regenerated plants. *Plant Cell Tissue Organ Cult.* **2019**, *138*, 339–351. [[CrossRef](#)]
43. Galbraith, D.W. Simultaneous flow cytometric quantification of plant nuclear DNA contents over the full range of described angiosperm 2C values. *Cytom. Part A J. Int. Soc. Adv. Cytom.* **2009**, *75*, 692–708. [[CrossRef](#)] [[PubMed](#)]
44. Mujib, A.; Malik, M.Q.; Bansal, Y.; Syeed, R.; Ejaz, B.; Mamgain, J. Somatic Embryogenesis in *Catharanthus roseus*: Proteomics of embryogenic and non-embryogenic tissues; and genome size analysis of regenerated plant. In *The Catharanthus Genome, Compendium of Plant Genomes*; Kole, C., Ed.; Springer: Cham, Switzerland, 2022; pp. 85–100. [[CrossRef](#)]
45. Doležel, J.; Greilhuber, J.; Suda, J. Estimation of nuclear DNA content in plants using flow cytometry. *Nat. Protoc.* **2007**, *2*, 2233–2244. [[CrossRef](#)] [[PubMed](#)]
46. Duncan, D.B. Multiple range and multiple F tests. *Biometrika* **1955**, *11*, 1478. [[CrossRef](#)]

Disclaimer/Publisher’s Note: The statements, opinions and data contained in all publications are solely those of the individual author(s) and contributor(s) and not of MDPI and/or the editor(s). MDPI and/or the editor(s) disclaim responsibility for any injury to people or property resulting from any ideas, methods, instructions or products referred to in the content.